RSC Advances

PAPER

View Article Online
View Journal | View Issue

Cite this: *RSC Adv.*, 2025, **15**, 5916

Construction of flexible paper-based sensor for label-free recognition of histamine in cow meat samples by conductive nano-silver ink: a new platform for the analysis of biogenic amines towards early diagnosis of meat spoil†

Rokhsareh Ebrahimi,[ab] Mohammad Hasanzadeh *[c] and Nasrin Shadjou [d]

Biogenic amines are organic nitrogen compounds that play key roles in various biological processes and are produced through amino acid decarboxylation. Among these, histamine stands out as a toxic biogenic amine with the potential to cause serious health issues when present at elevated levels in food, highlighting the importance of effective detection methods. However, current histamine detection approaches are often hindered by high costs, lengthy analysis times, and intricate procedures. This research introduces a novel, label-free method for detecting histamine in meat samples using highly conductive nano-silver inks to develop miniaturized sensors based on paper microdevice technology. The proposed paper-based electrochemical sensors offer significant advantages, including affordability, reproducibility, and environmental sustainability. A newly designed paper-based microsensor was developed for label-free histamine detection employing conductive nano-silver ink *via* a pen-on-paper technique. The fabrication process of the microsensor was thoroughly characterized through methods like field emission scanning electron microscope (FE-SEM), Energy Dispersive X-ray (EDAX), and Atomic Force microscopy (AFM). Key findings indicate that the microsensor successfully detects histamine concentrations across a broad dynamic range of 10 to 1000 nM, with a lower limit of quantification set at 10 nM. Validation of the sensor's performance was conducted using electrochemical tools such as cyclic voltammetry and square wave voltammetry, confirming its efficacy for real-time histamine monitoring in food products and biological environments. Additionally, the study underscores the sensor's excellent selectivity, long-term stability, and lightning-fast responsiveness, positioning it as a highly promising tool to enhance food safety and quality assurance.

Received 23rd December 2024
Accepted 18th February 2025

DOI: 10.1039/d4ra08965k

rsc.li/rsc-advances

1. Introduction

Food analysis is essential for health as it ensures the provision of nutrients needed for growth, energy production, and maintaining bodily functions, while also addressing chronic illnesses and health inequalities. This discipline involves examining the physical, biological, and chemical properties of food and evaluating their effects on health and disease. A key challenge for the food processing industry is managing food-borne illnesses linked to additives and contaminants. To address this, there is a critical need for fast, cost-effective, and accurate methods of analyzing these substances to reduce risks to public health.[1]

Biogenic amines are organic nitrogen compounds with hydroxyl, aromatic, and aliphatic structural bases that play an important role in biological processes. They have low molecular weight and are mainly produced by decarboxylation of free amino acids. In this process, the alpha-carboxyl group is removed from amino acids, resulting in the formation of various biogenic amines such as histamine from histidine, tyramine from tyrosine, and tryptamine from tryptophan.[2–5]

Biogenic amines are present in a wide range of food products such as fish, meat, dairy products, wine, beer, vegetables, fruits, nuts, and chocolates. They are beneficial at normal levels. They are important in neurotransmission, hormonal regulation, immune responses, and cell signaling.[6] However, if present in excess, they can cause food poisoning such as histamine poisoning as initiators of diverse physiological reactions and are considered potential carcinogens due to their ability to react with nitrite and form carcinogenic nitrosamines.[7] Therefore,

[a]*Nutrition Research Center, Tabriz University of Medical Sciences, Tabriz, Iran*
[b]*Asian Nano-Ink (ANI) company, Tabriz University of Medical Sciences, Tabriz, Iran*
[c]*Pharmaceutical Analysis Research Center, Tabriz University of Medical Sciences, Tabriz, Iran. E-mail: hasanzadehm@tbzmed.ac.ir*
[d]*Department of Nanotechnology, Faculty of Chemistry, Urmia University, Urmia, Iran*

† Electronic supplementary information (ESI) available. See DOI: https://doi.org/10.1039/d4ra08965k

they are of particular importance in food safety for consumers and can also be referred to as indicators of spoilage of some foods. Therefore, the detection of biogenic amines in foods is of particular importance due to their polarity and high solubility in water compared to organic solvents.[8]

Histamine (β-imidazolyl ethylamine) is one of the most toxic and active biogenic amines, whose health effects range from allergic reactions to food poisoning.[9] The acceptable concentration of histamine in food to ensure safety is less than 50 mg kg^{-1}, while levels above 200 mg kg^{-1} can cause poisoning and symptoms such as nausea and diarrhea, headache, bronchospasm, tachycardia, hypotension, urticaria, and nasal discharge.[10] Histamine levels therefore serve as vital indicators of freshness, safety, and quality of food. Improper storage of meat can lead to excessive production of histamine.[11] This is due to the action of endogenous decarboxylase enzymes on histidine, which is carried out by uncontrolled microbial activity during meat degradation.[12]

Several traditional methods/techniques have been used to determine Hist levels, including thin-layer chromatography,[13] fluorometric and colorimetric assays,[14] and gas chromatography.[15] Capillary zone electrophoresis, surface Raman scattering,[16] high-performance liquid chromatography,[17] chemical sensors,[18] and aptasensors.[19] While these methods offer high sensitivity and accuracy, they also have several limitations such as high instrumentation costs, time-consuming and complex sample preparation, and the need for trained specialists, and sensitivity to environmental interferences.[20] As a result, they are rarely used for on-site detection. With the increasing demand for monitoring toxicants in food, there is a need for a rapid, sensitive, and cost-effective method capable of detecting amines at ppb levels for the detection of histamine levels in real samples.

Sensor integration in food science and food chemistry is an emerging field that uses advanced technologies to improve the quality, safety, and processing of food. Smart sensors, often integrated with machine learning, are used in agriculture and food technology to increase food production and assess food quality. These sensors can track a variety of factors, including nutrient levels and pest detection, thereby supporting the production of high-quality food products. In the field of food chemistry, sensors are crucial for detecting chemical changes and ensuring food safety, especially through the use of nanosensors and other innovative materials.[2]

The integration of sensors into food science and chemistry has led to remarkable progress; however, challenges like the complexity of food matrices and the lack of standardization in sensor technology remain issues to address. Electrochemical methods offer straightforward and reliable analytical solutions, making them a superior alternative to traditional techniques for evaluating food quality and safety. The emergence of various nanomaterials has greatly contributed to the development of advanced electrochemical sensing devices, widely used in fields such as medical diagnosis, environmental monitoring, and food safety. Electrochemical sensors incorporating nanomaterials have gained notable attention due to their exceptional sensitivity and selectivity, real-time monitoring potential, and user-friendly nature.[3]

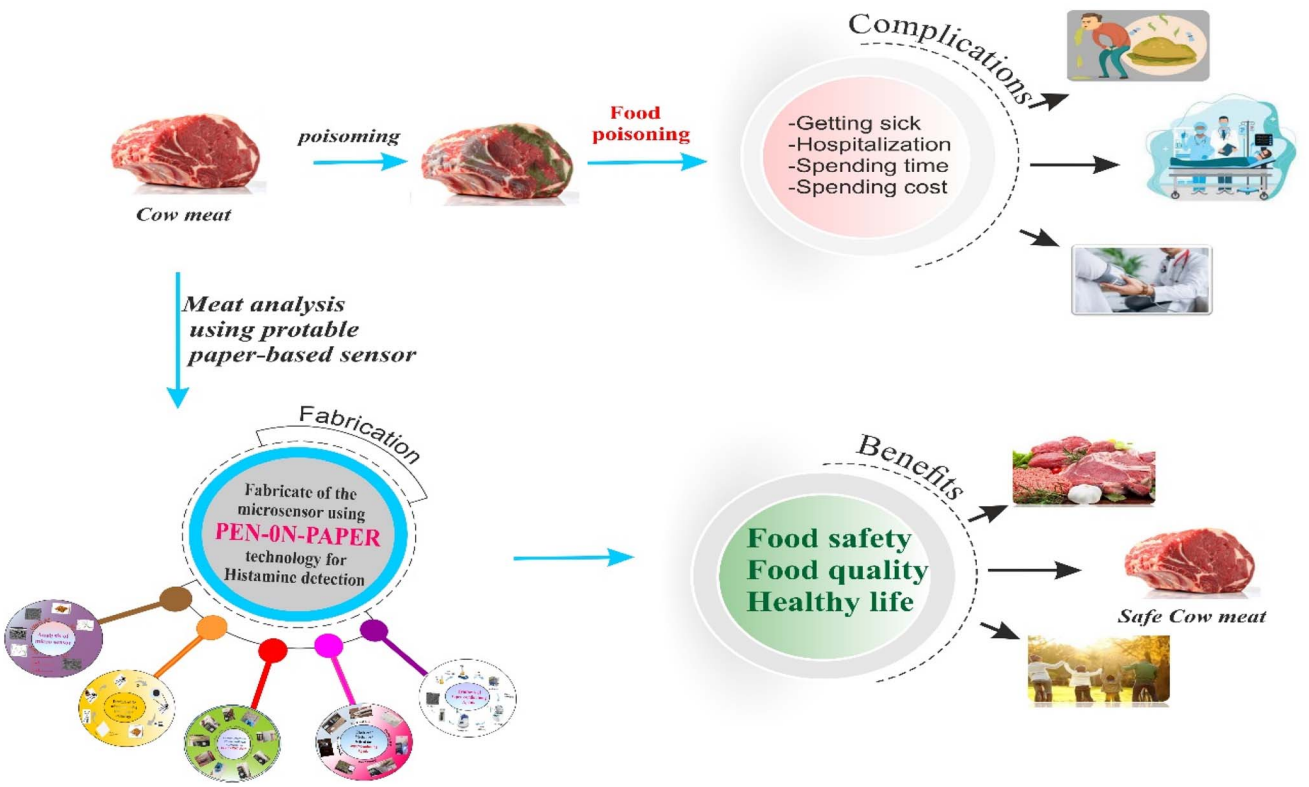

Scheme 1 Meat analysis using portable paper-based microscale sensor.

Paper sensors present a promising method for the precise detection of histamine. Integrating electrochemical sensor technology with compact paper-based micro-medical devices, such as nano-conductive Bernina-based paper electrodes, offers a practical solution for the initial analysis of food samples by both home users and the food industry across global supply chains. Cost-effective electrochemical microscale sensors serve as accessible diagnostic tools designed to identify specific compounds in various samples. Affordable paper-based electrochemical microscale sensors are extensively applied in a wide array of fields, from diagnosing medical conditions like diabetes, pregnancy, or urinary tract infections to monitoring environmental parameters such as pollutants in water, air, or soil. Additionally, these sensors play a crucial role in food safety, ensuring the detection of toxins and pathogens in food products, or in maintaining industrial standards by assessing the quality of raw materials and finished goods.[21]

This study presents an innovative label-free electrochemical microscale sensor designed for detecting histamine levels in raw beef, employing highly conductive nanoink and pen-on-paper technology as detection tools (Scheme 1). Paper-based platforms bring numerous advantages, including exceptional reproducibility, eco-friendliness, biodegradability, compatibility with microfluidics, minimal sample requirements, cost-effectiveness, ease of fabrication, inexpensive equipment usage, quick analysis, and potential for miniaturization. Consequently, utilizing paper-based sensors allows electrochemical techniques to remarkably enhance the sensitivity and accuracy of histamine detection in food, particularly in meat products.

This research introduces a groundbreaking approach for the label-free detection of histamine in meat samples by employing highly conductive nano-silver inks to develop compact sensors based on paper microdevice technology. The proposed paper-based electrochemical sensors boast significant advantages, including low cost, high reproducibility, and environmental sustainability. Utilizing conductive nano-silver ink and a pen-on-paper technique, a unique paper-based microsensor was designed for detecting histamine without the need for labeling. The sensor's performance was validated through electrochemical methods such as cyclic voltammetry and square wave voltammetry, confirming its effectiveness for real-time monitoring of histamine in food samples and biological systems. Additionally, the study emphasizes the sensor's excellent selectivity, long-term stability, and rapid response, establishing it as a highly promising tool for ensuring food quality and safety.

2. Experimental details

2.1. Reagents and materials

Histamine, Potassium ferricyanide $K_3Fe(CN)_6$, and potassium ferricyanide $K_4Fe(CN)_6$, were purchased from Sigma-Aldrich, Canada. Sodium hydroxide (NaOH), silver nitrate ($AgNO_3$), diacetate alcohol (DAA), sulfuric acid (H_2SO_4), polyacrylic acid (PAA), diethanolamine (DEA), glucose, cysteine (Cys), trichloroacetic acid (TCA), ascorbic acid (AA), dopamine (Dopa), uric acid (UA), proline (Pro), aspartic acid (ASP), methionine (Met), arginine (Arg), glycine (Gly) and urea were purchased from Merck, Germany. Deionized water was provided by Ghazi Pharmaceutical Company, Tabriz, Iran. All chemicals used were of the highest purity available unless stated otherwise.

2.2. Apparatus

EDS (Energy scattering spectroscopy) was employed to study chemical elements. A high-resolution field emission scanning electron microscope (FE-SEM) Hitachi SU8020, Czech with a 3 kV effectual voltage used for investigating the morphology of the electrode surface. The AFM images were obtained using a Bruker Dimension Icon microscope operating in ScanAsyst mode, utilizing OTESPA AFM probes (Bruker). For electrochemical measurements, a Palm Sense4c device (Palm Instruments, Utrecht, Netherlands) connected to a computer and analyzed by PS Trace software was used. The three-electrode system (reference, counter and working electrodes) was drawn on the surface of photographic paper using a pen containing synthesized conductive nano-silver ink (Fig. S1, see ESI†). The resistance of the synthesized nano silver ink was evaluated using an ohmmeter (XIOLE, XL830L, China, multimeter).

2.3. Preparation of meat samples

A 3 g slurry of meat sample was transferred into a centrifuge tube containing 10 mL of 5% (w/v) TCA and 200 μL of 1,7-diaminoheptane. The mixture underwent thorough vortexing for 15 minutes, followed by centrifugation at 5000*g* for 10 minutes at 4 °C. The supernatant obtained was carefully separated, while the residue underwent a second extraction using the same amount of TCA. The supernatants from both extractions were filtered through Whatman paper, combined, and the total volume was brought to 25 mL with TCA. For the analytical analysis, histamine was spiked into the meat samples following this protocol: 50 mg of muscle tissue was homogenized in 25 mL of 0.1 M PBS at pH 7.4. The homogenate was then centrifuged at 12 000 rpm for 30 minutes, and the supernatant was collected. It was subsequently diluted to 30 mL with water and stored at 4 °C in a refrigerator.

2.4. Synthesis of conductive nano-silver ink

To synthesize conductive nano-silver ink, 1.915 g of PAA and 40 g of DEA were initially dissolved in 65 wt% aqueous solutions and 50 g of water, respectively, before being combined. While stirring the mixture vigorously, approximately 20 g of $AgNO_3$ dissolved in 15 mL of H_2O was gradually introduced. The mixture ultimately turned black, signifying the successful formation of silver nanoparticles. The solution was then subjected to sonication at 65 °C for 1.5 hours. After cooling, 300 mL of ethanol was added as a mild solvent, and the sample was further concentrated *via* centrifugation at 9000 rpm for 20 minutes. The supernatant was discarded, and the collected precipitate was redispersed in 25 mL of water using vortexing and sonication. To eliminate excess PAA, the mixture was centrifuged again at 9000 rpm for 20 minutes, repeating the washing procedure three times. The refined product was then combined with 1.5 mL of water and filtered using a 10 μm polycarbonate membrane. Afterward, a 2 wt%

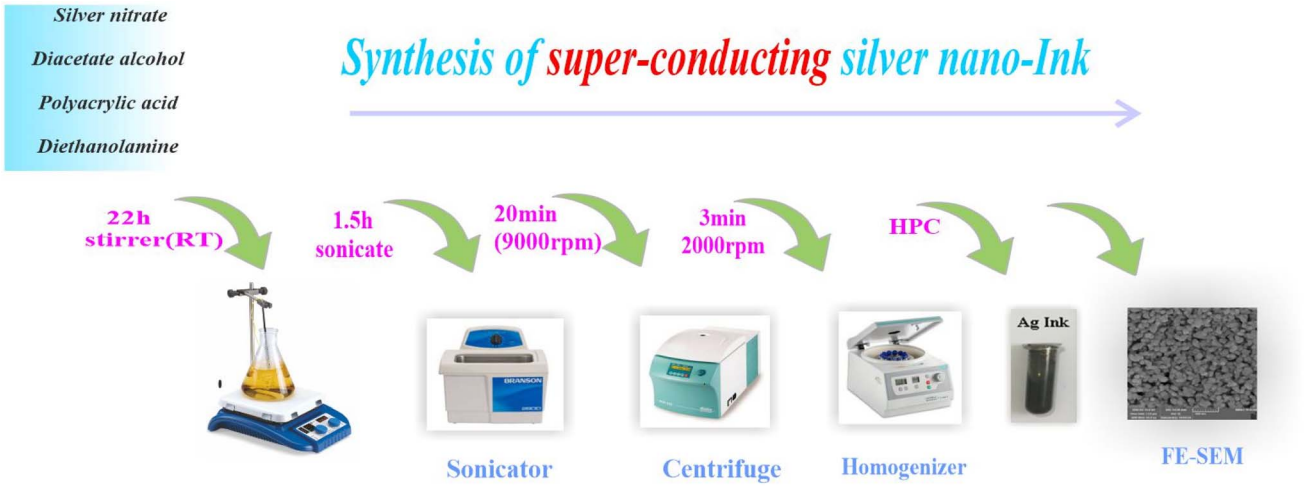

Scheme 2 Super-conductive Ag-nanoink preparation procedure.

hydroxypropyl cellulose solution prepared in a 1 : 1 (v/v) methanol-to-water mixture was added to the composite. Finally, the mixture was homogenized at 2000 rpm for 3 minutes. The entire procedure for preparing the conductive nano-silver ink is illustrated in Scheme 2 and Fig. S2 (see ESI†). The final homogenization and integration process involved mixing at a speed of 2000 rpm for 3 minutes.

2.5. Electrical and mechanical properties of the super-conducting conductive nano-silver ink

The electrical conductivity of the fabricated Ag highly conductive ink was demonstrated by successfully lighting up an LED, facilitated by the current flow from the anode to the cathode, thereby completing an electrical circuit. Additionally, its resistance was measured and verified using an ohmmeter (see Fig. S3A in the ESI†). The silver nanoink-based electrodes, deposited on cellulose substrates using pen-on-paper technology, were further investigated by drawing lines of varying thicknesses on paper. Measurements of electrical conductivity and resistance across all lines showed consistency, with no significant variation noted (see Fig. S3B in the ESI†). To assess the thermal performance of paper electrodes made from synthetic nanoink, temperature variations were monitored at 60, 100, and 150 °C. A digital hot plate with an aluminum-coated surface served to evaluate the thermal stress properties of the silver highly conductive ink, aiming to develop paper-based electronic writing. The aluminum coating acted as an insulating layer, protecting the microfluidic paper's surface from direct contact with the metal hot plate. The thermal stress evaluation was conducted following the application of the conductive ink *via* pen. Importantly, the electrodes dried immediately after application and did not require extended drying times or elevated temperatures, presenting a key advantage of the synthetic ink.

Notably, the electrodes dried instantly after being drawn, eliminating the need for prolonged drying times or elevated temperatures, which highlighted a key benefit of our synthetic ink. The paper electrodes were promptly applied to a digital screen following a 30 seconds drying period at 60, 100, and 150 °C (refer to the movie in ESI†). After resting for an additional 30 seconds, their electrical conductivity was analyzed using an LED, and their resistance measured 6.03 Ω as assessed with an ohmmeter in ohm units. Extended drying durations or exposure to higher temperatures had no effect on the electrodes' electrical conductivity or resistance. Interestingly, the ink-infused paper electrodes demonstrated a negative temperature coefficient effect, indicating an absence of resistance variation despite temperature increases. The exceptional interaction and effective bonding of the conductive nano-silver ink with the functional groups on the photographic paper contributed to the electrodes' stable resistance and remarkable conductivity when drawn with the electroconductive pen. Consequently, the silver nanoparticle-infused highly conductive ink exhibited outstanding electrical performance, even when subjected to baking temperatures exceeding ~150 °C (Fig. S3C, see ESI†).

The relative humidity test results demonstrate the capability of the microfluidic paper substrate to function as a responsive material for sensing silver ions. To evaluate the impact of humidity over time on the resistance and electrical conductivity of three silver nanoparticle-infused paper electrodes, the electrodes were prepared using a conductive pen. The electrical properties were then assessed at various intervals: the first electrode was tested immediately after water exposure, the second after ten minutes, and the third after thirty minutes post-wetting. It was found that the moisture absorbed by the ink had no effect on the electrical conductivity or resistance of the electrodes. Additionally, the LED maintained brightness at a resistance of 5.09 Ω for the electrodes (Fig. S3D in the ESI†).

The bending test was conducted to assess the mechanical flexibility of the paper-based electrode. The conductive lines, comprising conductive nano-silver ink layers deposited on a paper substrate, were repeatedly folded and unfolded for approximately 100 cycles. Depending on the position of the conductive layer, the sample experienced varying types of stress during the test. Specifically, during the folding process, the conductive layer on the paper surface underwent compressive

Scheme 3 Design electrodes on the different substrates by silver electrical pen.

and tensile strain. As detailed in Fig. S3 (refer to the ESI and Movie, ESI†), the paper exhibited excellent foldability without any visible cracks. Furthermore, it is noteworthy that beyond photographic paper, our electro-conductive pen is capable of crafting electrodes and drawing conductive lines on various surfaces, including latex gloves, glass, wood, double-sided tape, skin, ParaFilm, drywall, and notably, linen fabric. Resistance and electrical conductivity tests, illustrated in Scheme 3 and corresponding videos (refer to ESI), confirm the effectiveness of the synthetic ink on these substrates. These results collectively verify the suitability of our synthetic Ag highly conductive nano-ink for directly fabricating electrical circuits on diverse materials, including photographic paper, through the innovative pen-on-paper method.

3. Results and discussion

3.1. Fabrication of the paper-based electrochemical sensor using pen-on-paper technology

To fabrication the miniature paper electrode, the synthesized highly conductive nano-silver ink was manually applied onto the paper surface using a pen and dried almost instantaneously, within less than a second. Next, 5 μL of histamine was dispensed onto the sensing region of the paper electrode and allowed to incubate at room temperature for 20 minutes. Afterwards, electrochemical analysis was performed employing different techniques. During the experiments, the Ag ink electrodes and Ag/histamine ink electrodes acted as the working electrodes. All electrochemical experiments were carried out in a solution of $K_3[Fe(CN)_6]$ and $K_4[Fe(CN)_6]$ (5 mM), mixed in equal proportions, functioning as the redox probe. For SWV (square wave voltammetry) analysis, the working potential range was maintained between −1000 mV and +500 mV, using a scan rate of 10 mV. The steps involved in preparing the miniature paper-based electrochemical sensor for histamine detection are depicted in Scheme 4 and Fig. S4 (refer to ESI†).

3.2. Electrochemical preparation of the paper-based sensor

The electrochemical behavior of the fabricated microscale sensor was analyzed in two distinct phases. Fig. 1A and B illustrates the CV and SWV responses of the Ag nanoInk-based sensor in the presence of a 5 mM $K_3[Fe(CN)_6]/K_4[Fe(CN)_6]$ solution at a scan rate of 100 mV s^{-1}. Prior to histamine interaction, the electrode embedded with silver highly conductive ink exhibited a baseline current of 575 μA at a potential of 0.2 V.

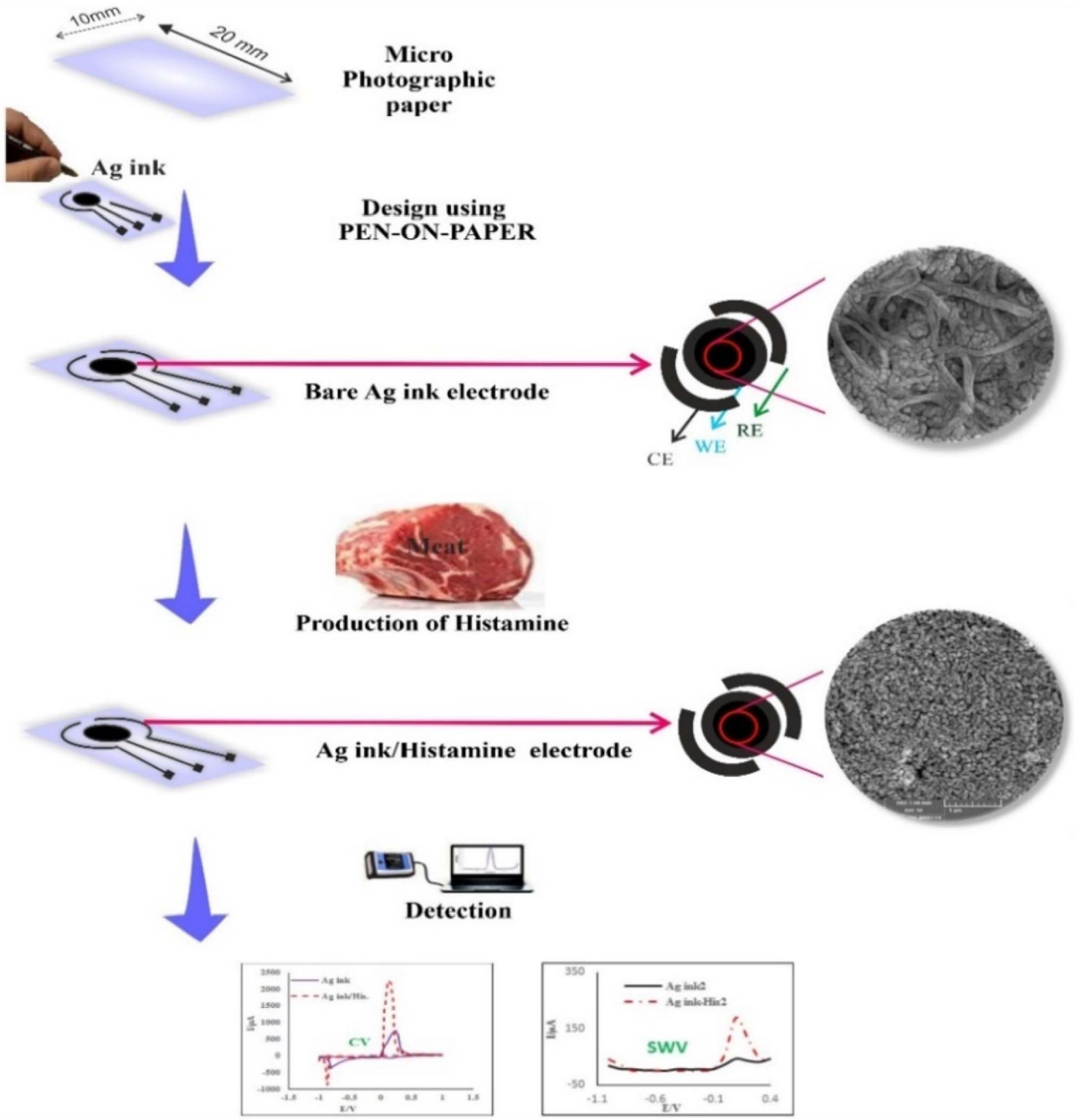

Scheme 4 The fabrication steps of the label-free electrochemical paper-based microscale sensor of histamine.

Upon subsequent exposure to histamine (500 nM), the Ag-Ink produced notable oxidation currents of 2030 μA at 0.1 V (refer to Table S1 in the ESI†). The pronounced negative anodic shift and the remarkable enhancement in current measurements confirm the appropriateness of the Ag-ink surface, as well as its exceptional capability, for histamine oxidation. The increased surface area afforded by the conductive nano-silver ink facilitates the permeation of histamine through the paper layer, thereby boosting the sensor's sensitivity. Moreover, the nanoparticles present on the surface of the photographic paper serve as binding sites for histamine's nitrogen groups, effectively expediting electron transfer with the 5 mM $K_3[Fe(CN)_6]$/$K_4[Fe(CN)_6]$ solution while providing a favorable platform for probe incubation. The superior oxidation stability, outstanding electrical conductivity, and advantageous surface properties of the Ag ink demonstrate its ability to significantly enhance electrochemical performance. The fast electron transfer rate and low charge transfer resistance characterize this electrode/electrolyte interface.

Silver nano-ink are known for their excellent conductivity and catalytic properties. When used in the modification of electrodes, they significantly improve the electrochemical

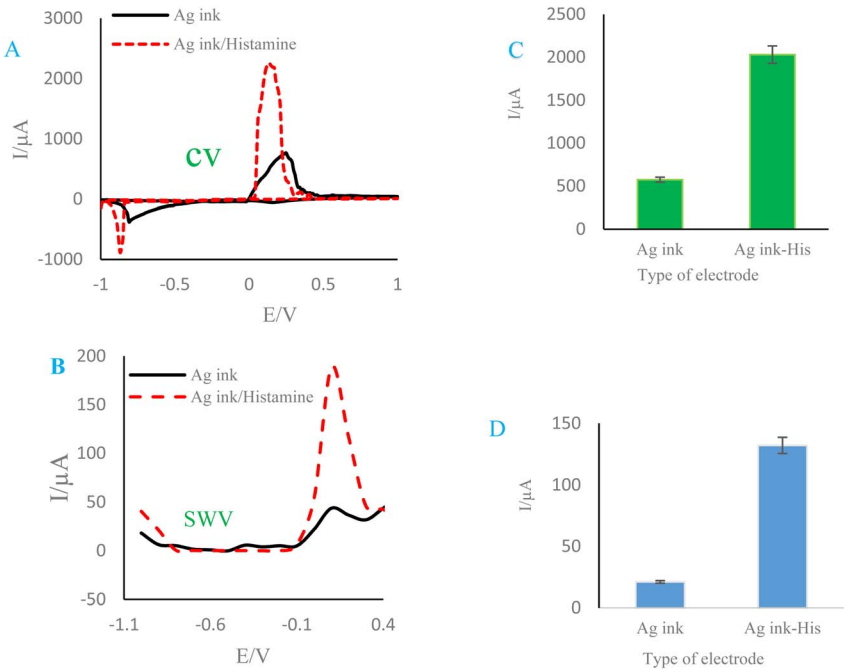

Fig. 1 (A and B) CVs and SWVs of paper modified conductive nano-silver ink and Ag ink/histamine in the presence of $K_3[Fe(CN)_6]/K_4[Fe(CN)_6]$ (5 mM) at the potential range of −1 to +1 V and sweep rate of 100 mV s^{-1}, respectively. (C and D) Histograms of peak current *versus* type of electrode obtained from CVs, SWVs respectively. (E) EIS of paper modified conductive nano-silver ink and Ag ink/histamine.

response due to their high surface area and the ability to facilitate charge transfer. The nanoparticles enhance the electron transfer kinetics, allowing for lower detection limits and faster response times when measuring histamine concentrations. This improved performance is particularly useful in applications where rapid detection is essential, such as food safety or clinical diagnostics (Scheme 5).

Also, EDAX spectra confirmed obtained results by electrochemical results (Fig. 2). As can be seen, before incubation of histamine on the surface of conductive nano-silver ink, intensity of C, N, Ag, are, 78.4, 17.8, 1997.1, respectively. Also, W% of C, N, Ag, are 8.60, 2.43, 82.54, respectively. Interestingly, after incubation of histamine on the surface of electrode, intensity of C reach to 110.6. Also, W% of C, reach to 9.56.

3.3. SEM and EDS characterization of histamine sensor

The morphological characteristics of the surfaces of various electrodes fabricated on the sensor were analyzed using FE-SEM, EDS, Cross-SEM, and AFM imaging techniques. (Fig. S5 in the ESI†) for the FE-SEM images illustrating the fabricated conductive nano-silver ink and Ag ink/histamine paper electrodes for surface analysis. A noticeable change in the optical appearance of the paper substrate was detected following the deposition of nanoparticles and incubation of histamine. After the chemical reduction process, the surfaces of photographic paper fibers appeared coated with a uniform, thin conductive nano-silver ink layer, which fused to form a continuous structure. The FE-SEM images revealed the silver nanoparticles as spherical particles with a consistent architecture. Additionally, it was evident that the nanoparticles were densely integrated within the fibers of the photographic paper. Upon further examination of cross-sectional images under higher magnification (Fig. 3), the silver nanoparticles (approximately 50 nm in diameter) were observed to interconnect within the fibers, creating an interconnected, interpenetrating network.

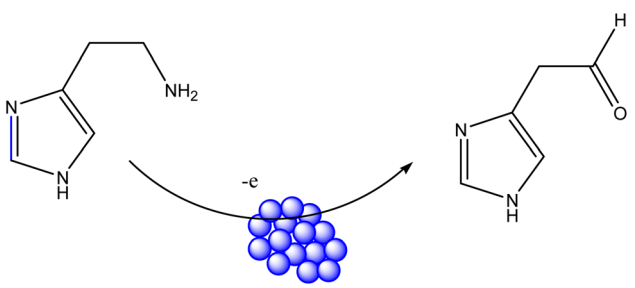

Scheme 5 Detection mechanism of histamine using conductive nano-silver ink paper-based sensor.

The interaction between the paper's functional groups and the ink facilitates the formation of a uniform layer on the surface, making it well-suited for immobilizing biological agents. The absence of nanoparticle aggregation on the paper's surface, along with their complete penetration into the fibers, demonstrates the substrate's efficiency and strong immobilization of silver nanoparticles on the surface. This leads to high bulk conductivity, significantly enhancing electrical conductivity and enabling the creation of electrical circuits directly on the paper fibers, alongside the development of a highly conductive sensor for various applications. Following the assembly of histamine on the electrode, visible changes in surface morphology suggest successful histamine immobilization. The paper fibers become obscured due to the higher

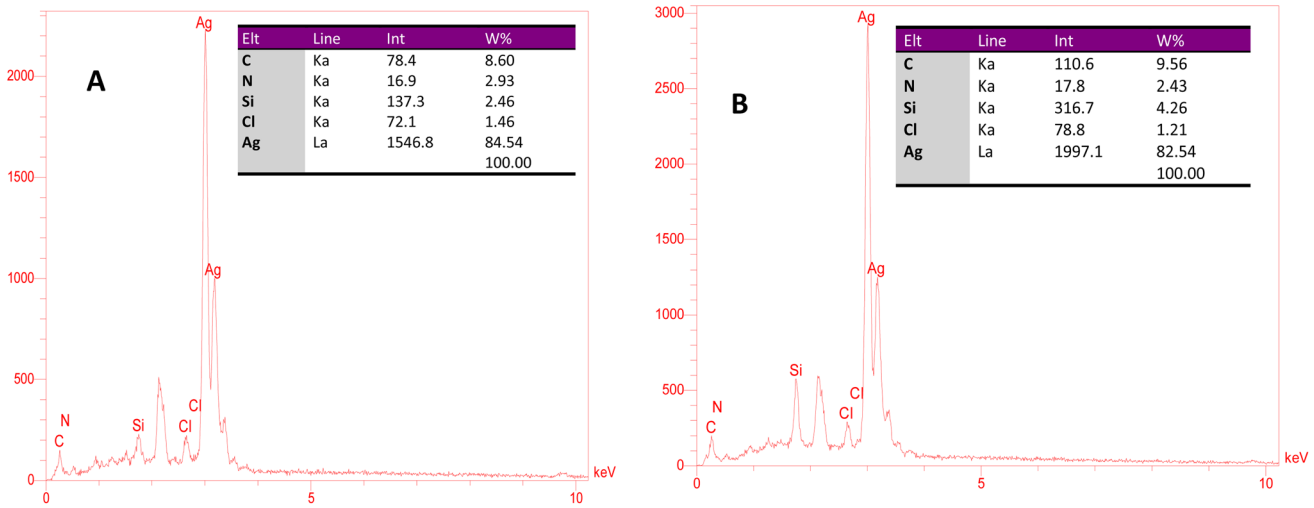

Fig. 2 EDAX spectra of microelectrode prepared by conductive nano-silver ink before (A), after incubation with histamine (B).

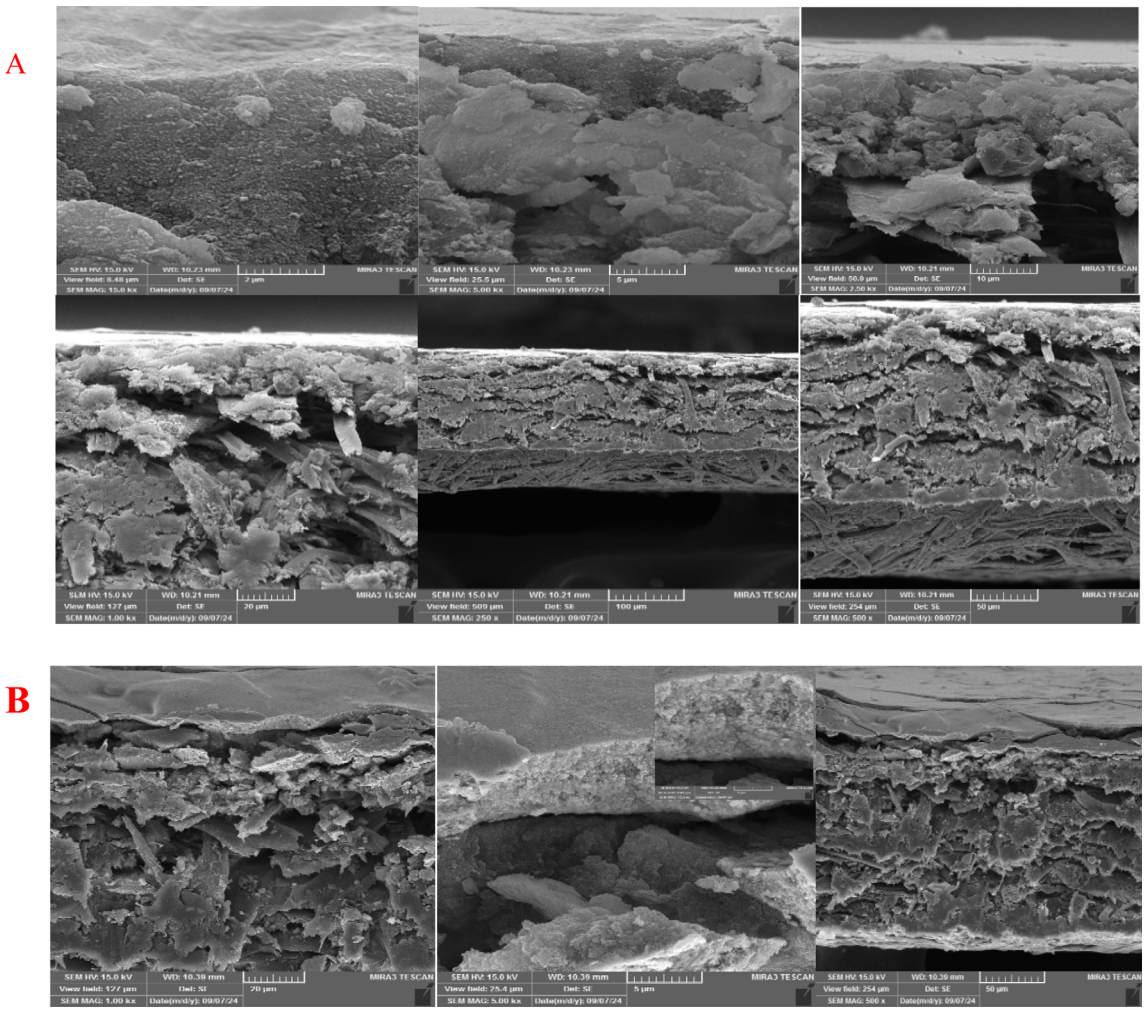

Fig. 3 Cross FE-SEM images of microelectrode prepared by conductive nano-silver ink before (A), after incubation with histamine (B) at various magnifications.

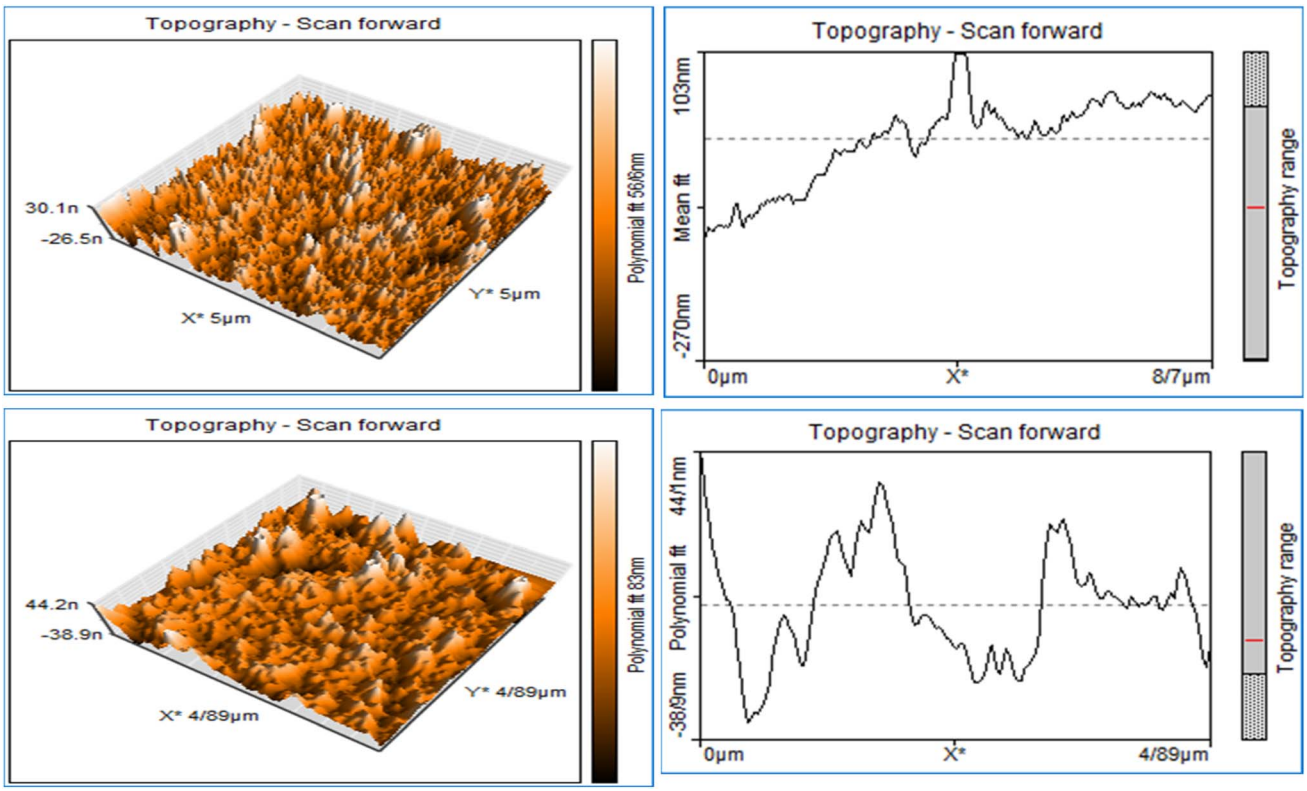

Fig. 4 Topographical AFM images of microelectrode prepared by conductive nano-silver ink before, after incubation with histamine along with roughness curves.

accumulation of histamine, further confirming the attachment of histamine on the silver-inked microphotograph paper. Cross-sectional FE-SEM images additionally validate the distinction between two electrode surfaces and prove the effective assembly of histamine. Moreover, a semi-quantitative estimation of the surface composition *via* EDX analysis (Fig. S6, referenced in the ESI†) revealed that the initial paper surface was covered by 82.5% (wt%) elemental silver. However, after histamine assembly, the elemental silver content was reduced, attributed to surface coverage with histamine.

The topographical characteristics of the paper microelectrodes' surface were analyzed *via* AFM. Surface morphology and electrochemical properties of histamine microsensors were examined to investigate the structure of both the untreated and histamine-coated electrodes using the AFM technique, facilitating a detailed examination of the highly conductive nanoparticle substrate. For this analysis, the average roughness (R_q) was measured at various stages of electrode modification, both prior to and following histamine treatment, with surface topologies evaluated throughout each phase. The findings revealed that the silver ink electrode's surface initially displayed an R_q of 56.6 nm. Upon histamine treatment, the average roughness increased to an R_q of 83 nm, as illustrated in Fig. 4. Moreover, FE-SEM analysis indicated that all nanoparticles were distributed into distinct nanoclusters. After the application of histamine, the surface morphology showed significant alterations, yielding consistent results and verifying the successful immobilization of histamine on the electrode surface. Electrodes modified through this approach demonstrate the capability to detect lower concentrations of histamine effectively.

3.4. Analysis of the microscale sensor performance

The performance of the engineered microscale sensor in detecting varying concentrations of histamine was assessed. To achieve this, histamine standard solutions at concentrations of 10, 50, 100, 200, 400, 600, 800, and 1000 nM were immobilized onto the silver-ink surface and analyzed using the SWV technique in a 5 mM $K_3[Fe(CN)_6]/K_4[Fe(CN)_6]$ solution. Fig. 5 illustrates the SWV results obtained from the analysis of different histamine concentrations in the standard samples using a scan rate of 100 mV s^{-1}. Additionally, the calibration curve for these concentrations, depicted in Fig. 5, demonstrates a linear detection range between 10–1000 nM and a lower limit of quantification (LLOQ) of 10 nM. The peak current consistently increases as histamine concentration rises, validating the functionality of the sensor, which operates on a bright signal mechanism. The linear regression equation utilized to generate the calibration curve for SWV establishes a quantitative relationship between the measured current and the histamine concentration in the standard samples.

$$I\ (\mu A) = 3.2127 C_{\text{histamine}}\ (\text{nM}) + 990.6,\ R^2 = 0.9963.$$

The results obtained highlight the remarkable efficiency of the fabricated paper-based electrochemical microscale sensor

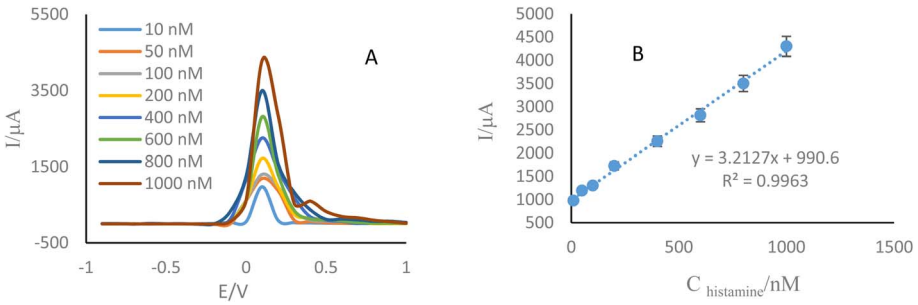

Fig. 5 (A) SWVs of the engineered sensor (Ag ink/Ag ink) in different concentrations of histamine (10, 50, 100, 200, 400, 600, 800, 1000 nM). (B) Relationship between I_{pa} and histamine concentration in standard sample. $t_{eq} = 2$, $E_{being} = -1$ V, $E_{end} = 1$ V, $E_{step} = 0.1$ V, amplitude = 0.001 V, frequency = 10 Hz using $K_3[Fe(CN)_6]/K_4[Fe(CN)_6]$ (5 mM) as the supporting electrolyte.

for detecting histamine at low concentrations. This biosensor stands out for its simplicity and ease of use, eliminating the need for advanced or complicated equipment while ensuring rapid detection. Furthermore, its compact design enhances portability, making it highly convenient.

Based on the results obtained, the developed microscale sensor exhibited impressive analytical performance. The findings suggest that the proposed sensor offers rapid analysis (under 2 minutes), a high active surface area attributed to the silver ink, outstanding electrical conductivity, stability, and strong reactivity with biological components, making it an efficient platform for histamine detection in biological samples. Moreover, a comparison between our synthetic ink and previously developed conductive ink composites reveals that our ink provides an extensive surface area, which enhances the analyte's charge density. Consequently, the engineered device demonstrates the capability to measure histamine at nanomolar concentrations with exceptional sensitivity. Importantly, the proposed platform significantly reduces analysis time in comparison to other studies. Another notable advantage of this microscale sensor, relative to other biosensors, lies in its rapid and effective analytical capacity, positioning it as a potential alternative to traditional detection techniques. Overall, this biosensor's remarkable analytical features make it a highly promising tool for future analyte detection.

3.5. Real sample analysis

To conduct label-free electrochemical detection of histamine as a biogenic amine, a paper-based microscale sensor coated with conductive nano-silver ink was utilized without prior drying. The sample, consisting of a mixture of histamine analyte and spoiled meat, is applied directly onto the microscale sensor's surface, followed by the recording of square wave voltammograms (SWVs). The resulting voltammograms are then analyzed for evaluation purposes. In the final assessment and quantification step, FDA guidelines are referenced to determine the presence of histamine. Key parameters such as the linear response range, detection limit, and quantification limit, along with validated data, will be derived and documented. A comparison with current standard techniques like HPLC will also be performed to align the analytical results and confirm the reliability of the proposed method.

The designed microscale sensor was applied to detect histamine levels in meat samples. To accomplish this, varying concentrations of histamine and meat samples were prepared by diluting them in a 1 : 1 (v/v) ratio, and 5 μL from each was deposited onto the surface of the engineered microelectrode (Ag ink/histamine) for incubation. As illustrated in Fig. 6A, the results of the SWVs for the sensor were obtained using $K_3[Fe(CN)_6]/K_4[Fe(CN)_6]$ (5 mM) as the electrolytic medium. The

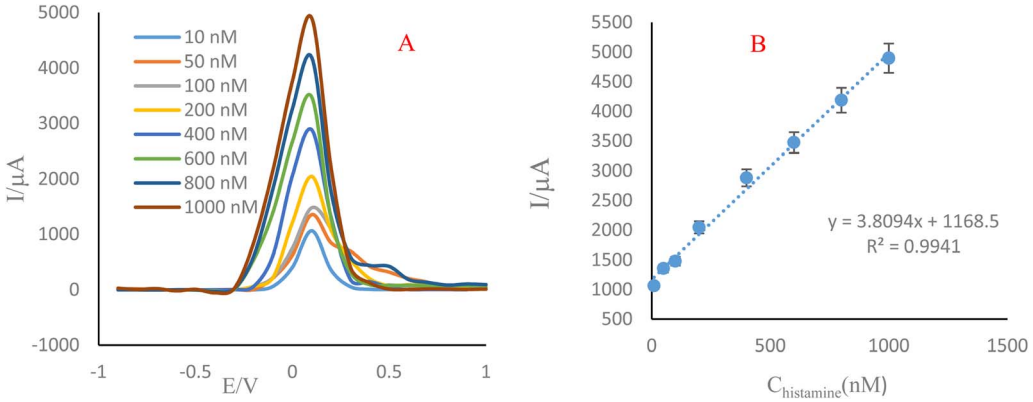

Fig. 6 (A) SWVs of the engineered sensor in different concentrations of histamine biomarker (10, 50, 100, 200, 400, 600, 800 and 1000 nM). (B) Relationship between I_{pa} and histamine concentration in meat sample. $T_{eq} = 2$, $E_{being} = -1$ V, $E_{end} = 1$ V, $E_{step} = 0.1$ V, amplitude = 0.001 V, frequency = 10 Hz using $K_3[Fe(CN)_6]/K_4[Fe(CN)_6]$ (5 mM) as the supporting electrolyte.

corresponding calibration curve, depicting the relationship between peak current variations and histamine concentration in the meat samples, is presented in Fig. 6B. The sensor exhibited a lower limit of quantification (LLOQ) of 10 nM, with a linear detection range spanning from 10 to 1000 nM. The linear correlation between the SWVs signal and histamine concentration can be described by the equation I (μA) = $3.8094C_{\text{histamine}}$(nM) + 1168.5, with an R^2 of 0.9941. Based on these findings, the proposed microscale sensor demonstrates effectiveness and reliability for identifying histamine in meat samples.

Table 1[22–43] present a comparison of the analytical techniques employed in the current study with other similar methods for histamine quantification in real samples. The findings demonstrate that the method developed in this research offers several key advantages, including a significantly shorter electrode fabrication time (30 minutes compared to 72 hours), reduced cost (0.5$ *versus* 60$), high flexibility due to its bendable design, use of non-toxic materials (conductive ink instead of highly hazardous solvents), fast analysis time (only 1 minute compared to 1–4 hours), portability linked to its miniaturized structure and lightweight design (0.05 g), as well as excellent stability in high-temperature (~100 °C) and wet conditions with a straightforward fabrication process. Furthermore, when contrasted with traditional techniques like HPLC, CE, and GC/MS/MS, our engineered sensor demonstrates additional advantages. These include real-time and *in situ* analysis, the elimination of the need for costly instrumentation or expert users, applicability to personalized medicine and point-of-care testing (POCT), as well as offering high accuracy coupled with appreciable sensitivity and selectivity. Remarkably, this study represents the first reported use of paper-based microelectrodes containing silver highly conductive ink as a support platform for histamine determination in meat samples. Overall, our approach is proposed as a robust and reliable method for accurately quantifying biogenic amines in real-world applications.

3.6. Determination of histamine in real samples

To assess the capability of the developed microscale sensor in detecting histamine within real samples, its performance was tested on meat samples using the SWV method with $K_3[Fe(CN)_6]/K_4[Fe(CN)_6]$ (5 mM) as the supporting electrolyte. For this analysis, 5 μL of a centrifuged meat extract was combined with varying concentrations of histamine and applied to the surface of a silver ink paper electrode for incubation. Subsequently, calibration curves were constructed by plotting the peak current against the histamine concentration in meat samples (Fig. 7A). A calibration curve showing the relationship between peak current changes and histamine concentration in the meat is presented in Fig. 7B. The sensor exhibited a lower limit of quantification (LLOQ) of 10 nM, with a linear detection range from 10 to 1000 nM. The SWV's linear response to histamine concentration followed the expression I (μA) = $2.9382C_{\text{histamine}}$ (nM) + 1613.7, with R^2 = 0.9973. Based on these findings, the proposed microscale sensor demonstrates strong suitability for histamine detection in meat samples.

Various analytical methods (Table 1) have been outlined for detecting histamine across diverse matrices and are acknowledged for their superior sensitivity and broad applicability in quantifying histamine within biological samples. These methods are favored due to their reliability, reproducibility, speed of analysis, and high sensitivity. However, they are not without drawbacks, as they often involve limited sensitivity, labor-intensive and protracted extraction procedures, complex workflows, and significant costs. In this study, we propose the development of a paper-based electrochemical microsensor utilizing highly conductive ink as an efficient alternative to these cumbersome analytical approaches for the accurate quantification of histamine in meat samples. Our method, when compared to existing techniques, exhibits an extended linear range for the calibration curve, a lower limit of quantification (10 nM), and several additional benefits: it delivers faster results, is cost-efficient, boasts a low detection limit, and is eco-friendly.

4. Analytical method validation

4.1. Selectivity

Selectivity is a key parameter in the performance analysis of a biosensor. It represents the sensing probe's capacity to accurately differentiate the target analyte from other non-specific substances. In the case of histamine-a biogenic amine found in food that coexists with other amines—it is essential to evaluate the proposed microscale sensor's ability to selectively detect histamine against these compounds. The sensor's detection proficiency was assessed using the SWV technique in the presence of potential interfering species, including the amino acids Cys, AA, Dopa, UA, Pro, ASP, Met, Arg, Gly, and glucose. As depicted in Fig. S7 (refer to the ESI†), the presence of these interferents did not significantly influence the absorption rate of histamine, confirming the sensor's robustness. Furthermore, Table S2 (also in the ESI†) presents a comparative analysis of current intensity and potential for the various interferences, where only negligible variations in peak current were observed. Consequently, the developed electrochemical microscale sensor demonstrates high selectivity and is well-suited for histamine detection in complex food matrices.

4.2. Intra-day stability of microscale sensor

For practical implementation, ensuring the stability of the proposed sensor is essential. To evaluate daily stability, a single electrode was stored in a refrigerator for four days while square wave voltammograms (SWVs) were recorded. The electrochemical performance of the fabricated microscale sensor was studied by measuring SWVs in a 5 mM solution of the supporting electrolyte, $K_3[Fe(CN)_6]/K_4[Fe(CN)_6]$. As illustrated in (Fig. S8, refer to ESI†), the electrode's peak current intensity measured 1805 μA on the first day but dropped to 1716 μA on the second day. A further decline in current intensity was observed over subsequent days. These findings suggest that the

Table 1 Performance comparison of developed microscale sensor with other previously reported sensors for histamine detection in real samples

Working electrode/applied material or surface	Type of method/technique	Type of real sample	Linear range	LOD/LOQ/LLOQ	Ref.
Conductometric detection (cITP-CZE-COND)	Electrophoresis	Foodstuffs and feedstuffs	(22–222 ng mL^{-1})	4 ng mL^{-1}	22
Molecularly imprinted solid-phase extraction		Foods	0.1–100.0 μg L^{-1}	0.087 μg L^{-1} and 0.29 μg L^{-1}	23
Silica capillary		Tuna fish	1–102 mg L^{-1}	0.14 mg L^{-1}	24
Paper electrophoresis		Fish and seafood	30 to 1000 ng	(1.5 mg/100 g)	25
Visible (HPLC-UV) and mass spectrometry (MS)	High performance liquid chromatography (HPLC)	Food	0.2 to 1.0 lg mL^{-1}	0.2 lg mL^{-1}	26
(9-Flourenilmethyl chloroformate (FMOC-Cl))		Food	0.16–5.00 μg mL^{-1}	0.16 μg mL^{-1}	27
Under the EU regulation		Fish and fishery products	(1–250 mg kg^{-1})	(1.00 mg kg^{-1})	28
Not reported	(TLC)	Fish and fishery products	30 ng to 1000 ng	(2.0 mg/100 g)	29
	Colorimetric	Fish flesh	0–100 μg mL^{-1}	Not reported	30
Gold nanoparticles with dual sensor system	UV-vis and fluorescence	Food	UV-vis(0.001–10.0 mM) and fluorescence (0.01–1.0 μM)	UV-vis(0.87 nM) and fluorescence and (2.04 nM)	31
Nanoporous alumina membrane	Electrochemical	Seafood	1–100,000 μM	0.003 μM	32
Screen-printed carbon electrode		Fish and shrimps	2.5–125 μM 125–400 μM	1.181 μM	33
Apt/AuNFs/ITO		Crab	1 to 5000 nM	0.79 nM	34
Nano-TiO_2/FTO		Food	10^{-7}–10^{-2}M	4.6 × 10^{-8} mol L^{-1}	35
Single-walled carbon nanotubes (SWCNTs)		Fish	0.005 to 50 ng mL^{-1}	0.005	36
PS/GONC/GCE		Fish	0.1–3 μM	0.03 μM	37
Carbon paste and screen-printed carbon		Fish sauce	Up to 10 mg L^{-1}	0.2 mg L^{-1}	38
Graphene and platinum		Freshwater fish	0.1–300 μM	25.4 nM	39
Ceria-Polyaniline (CeO_2-PANI)		Tiger prawn	132.4 μM	48.7 μM	40
AuNPs		Sardine	2.0–100 μM	0.6 μM	42
SPCE		Chicken meat	10–300 mmol L^{-1}	3.0 mmol L^{-1}	43
Conductive nano-silver ink	SWV	Cow meat	10–1000 nM	10 nM	This work

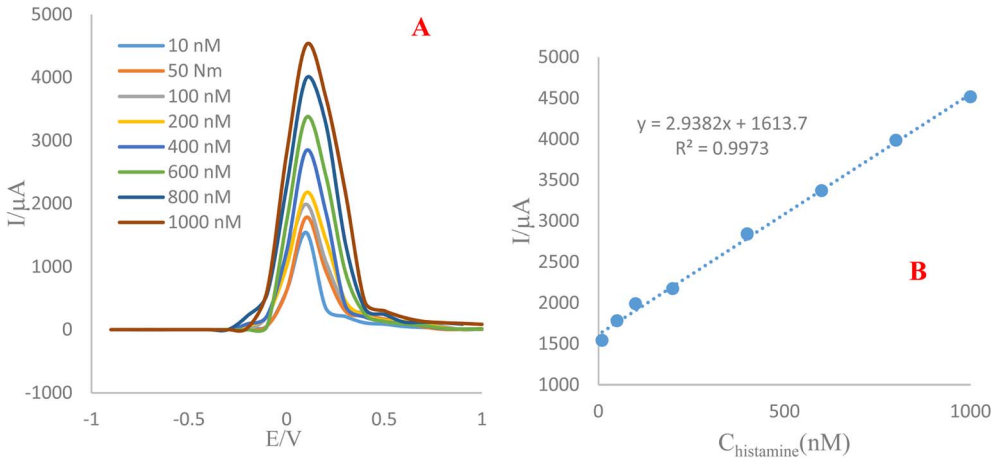

Fig. 7 (A) SWVs of the engineered sensor in different concentrations of histamine biomarker (10, 50, 100, 200, 400, 600, 800 and 1000 nM). B) Relationship between I_{pa} and histamine concentration in meat sample. $T_{eq} = 2$, $E_{being} = -1$ V, $E_{end} = 1$ V, $E_{step} = 0.1$ V, amplitude = 0.001 V, frequency = 10 Hz. Using $K_3[Fe(CN)_6]/K_4[Fe(CN)_6]$ (5 mM) as the supporting electrolyte.

sensing efficiency diminishes over time, as the prepared electrodes are unable to maintain stability across multiple days, as reflected in the variance in current between the initial and subsequent measurements.

4.3. Inter-day stability of microscale sensor

The main objective of sensor research is to design more stable and reliable sensors for environmental applications. The inter-day stability of the microscale sensor was analyzed throughout the day using the SWV technique within a voltage range of −1 to +1 V. Under comparable conditions, measurements were performed daily at one-hour intervals while the sensor was kept at 4 °C. The findings revealed a slight decline in current intensity after one hour. This suggests that, despite the sensor demonstrating moderate stability, its performance diminishes over time (Fig. S9, ESI†).

4.4. Reproducibility of the electrochemical sensor

To evaluate repeatability, the performance of three paper-based electrodes fabricated using silver ink through the SWV technique was assessed after introducing histamine at concentrations of 50, 250, and 500 nM in a 5 mM $K_3[Fe(CN)_6]/K_4[Fe(CN)_6]$ solution (Fig. 8). The results indicate that the developed electrochemical microscale sensor for histamine exhibits strong repeatability and stability. The calculated standard deviations (SD) for histamine concentrations of 50, 400, and 1000 nM were 2.33%, 3.04%, and 2.9%, respectively, highlighting the sensors' precision (Table S3, detailed in the ESI†).

4.5. Reproducibility of the sensor with three different concentrations

To evaluate the reproducibility of the microscale sensor designed for histamine detection, the square-wave voltammetry (SWV) technique was utilized within a potential range of −1 to 1 V at a scan rate of 100 mV s^{-1}. To begin, 50 nM of histamine was deposited onto the surfaces of three separate electrodes. To verify consistency, another three sensors were tested with a histamine concentration of 400 nM under the same conditions, followed by a third group of three sensors tested using

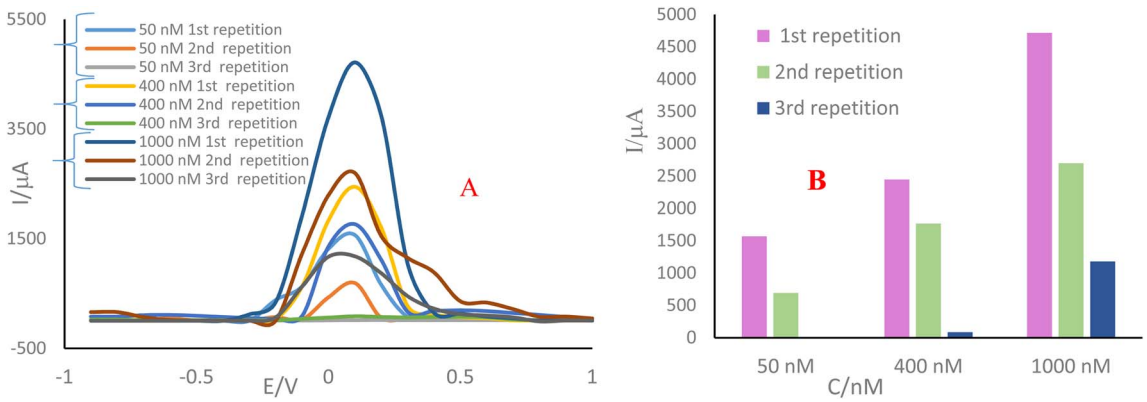

Fig. 8 (A) Three consecutive SWVs of the three microscale sensor drop cast by various concentrations of histamine (50, 400, and 1000 nM). The supporting electrolyte was 10 mL of $K_3[Fe(CN)_6]/K_4[Fe(CN)_6]$ (5 mM) solution, potential range: −1 to 1 V, Sweep rate = 100 mV s^{-1}. (B) Corresponding histogram.

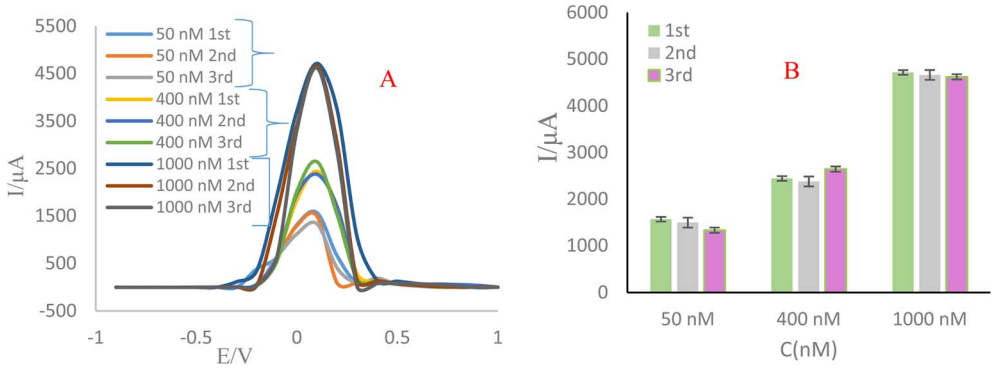

Fig. 9 (A) The first, second, and third SWVs of the three individual microscale sensor with three different concentrations of histamine (50, 400, and 1000 nM). The supporting electrolyte was 10 mL of $K_3[Fe(CN)_6]/K_4[Fe(CN)_6]$ (5 mM) solution, SR = 100 mV s^{-1}. (B) Corresponding histogram.

1000 nM histamine. The results indicated that all electrodes produced comparable current intensities across the different histamine concentrations, highlighting both the method's reliability and reproducibility (Fig. 9). Furthermore, analysis of the standard deviations (SD) for 50, 250, and 500 μM, which were determined as 3.3%, 4.2%, and 1.2% respectively, reinforced the sensors' accuracy (Table S4, see ESI†).

5. Conclusion

This research represents the first instance of employing a highly conductive nano-silver ink combined with a pen-on-paper technology approach to design and examine a novel label-free electrochemical microscale sensor. This innovative sensor demonstrates high affinity and specificity for the rapid and sensitive detection of histamine in meat samples. The developed microscale sensor offers notable advantages, including exceptional conductivity, consistency, and flexibility, making it a strong candidate for practical applications in food safety diagnostics. The findings revealed that the sensor accurately detects histamine concentrations ranging from 10 nM to 1000 nM, with a lower limit of quantification (LLOQ) of 10 nM. Consequently, this microscale sensor is efficient for quantifying histamine in food samples, exhibiting a low limit of detection (LOD), a broad linear detection range, superior selectivity, and robust stability. Electrochemical techniques such as cyclic voltammetry and square-wave voltammetry were utilized to validate the sensor's performance, showcasing its potential for real-time monitoring of histamine levels in diverse samples. Despite its promising functionality, this study highlights challenges related to substrate stability and underscores the need for continued research to identify advanced materials that can improve the durability and performance of the microscale sensor. These findings hold significant promise for the future integration of paper-based microsensors in detecting biogenic amines and other biomarkers in complex sample matrices.

Data availability

Access to the data used in this study is available upon request and may be subject to approval by the data provider. Restrictions may apply to the availability of these data, which were used under license for this study. Interested parties are encouraged to contact the corresponding author for further information on accessing the data. All relevant data supporting the findings of this study are available within the article and its ESI files,† or from the corresponding author upon reasonable request. Access to some data may be restricted due to privacy or ethical restrictions. Any restrictions to data availability will be disclosed at the time of data request.

Conflicts of interest

There are no conflicts to declare.

Acknowledgements

This work is based upon research funded by Tabriz University of Medical Science under project No. 75828. Also, authors thanks from Urmia University and Tabriz university of medical science for instrumental support.

References

1 F. Mustafa and S. Andreescu, Chemical and biological sensors for food-quality monitoring and smart packaging, *Foods*, 2018, **7**(10), 168.
2 M. S. Thakur and K. V. Ragavan, Biosensors in food processing, *J. Food Sci. Technol.*, 2013, **50**, 625–641.
3 V. S. Manikandan, B. Adhikari and A. Chen, Nanomaterial based electrochemical sensors for the safety and quality control of food and beverages, *Analyst*, 2018, **143**(19), 4537–4554.
4 P. Visciano, M. Schirone and A. Paparella, An overview of histamine and other biogenic amines in fish and fish products, *Foods*, 2020, **9**(12), 1795.
5 A. Durak-Dados, M. Michalski and J. Osek, Histamine and other biogenic amines in food, *J. Vet. Res.*, 2020, **64**(2), 281–288.
6 N. Sanlier and M. Bektesoglu, Migraine and biogenic amines, *Ann. Med. Health Sci. Res.*, 2021, (4), 1362–1371.

7 A. K. Omer, R. R. Mohammed, P. S. Ameen, Z. A. Abas and K. Ekici, Presence of biogenic amines in food and their public health implications: A review, *J. Food Prot.*, 2021, **84**(9), 1539–1548.
8 M. Moniente, L. Botello-Morte, D. García-Gonzalo, R. Pagán and I. Ontañón, Analytical strategies for the determination of biogenic amines in dairy products, *Compr. Rev. Food Sci. Food Saf.*, 2022, (4), 3612–3646.
9 A. C. Anithaa, S. B. Mayil Vealan, G. Veerapandi and C. Sekar, Highly efficient non-enzymatic electrochemical determination of histamine based on tungsten trioxide nanoparticles for evaluation of food quality, *J. Appl. Electrochem.*, 2021, **51**, 1741–1753.
10 L. Maintz and N. Novak, Histamine and histamine intolerance, *Am. J. Clin. Nutr.*, 2007, **85**(5), 1185–1196.
11 A. Durak-Dados, M. Michalski and J. Osek, Histamine and other biogenic amines in food, *J. Vet. Res.*, 2020, **64**(2), 281–288.
12 G. Wu, X. Dou, D. Li, S. Xu, J. Zhang, Z. Ding and J. Xie, Recent progress of fluorescence sensors for histamine in foods, *Biosensors*, 2022, **12**(3), 161.
13 H. Yu, D. Zhuang, X. Hu, S. Zhang, Z. He, M. Zeng, X. Fang, J. Chen and X. Chen, Rapid determination of histamine in fish by thin-layer chromatography-image analysis method using diazotized visualization reagent prepared with p-nitroaniline, *Anal. Methods*, 2018, **10**(27), 3386–3392.
14 A. Phoungsiri, N. Lerdpiriyaskulkij, A. Mathaweesansurn and E. Detsri, Ultrasonic-driven chemical reduction synthesis of alizarin complexone-modified gold nanoparticles for dual-signal colorimetric and fluorometric sensing of histamine in seafood products, *Talanta*, 2024, **280**, 126703.
15 M. Kamankesh, A. Mohammadi, A. Mollahosseini and S. Seidi, Application of a novel electromembrane extraction and microextraction method followed by gas chromatography-mass spectrometry to determine biogenic amines in canned fish, *Anal. Methods*, 2019, **11**(14), 1898–1907.
16 L. Vitali, A. C. Valese, M. S. Azevedo, L. V. Gonzaga, A. C. Costa, M. Piovezan, J. P. Vistuba and G. A. Micke, Development of a fast and selective separation method to determine histamine in tuna fish samples using capillary zone electrophoresis, *Talanta*, 2013, **106**, 181–185.
17 Z. Wang, J. Wu, S. Wu and A. Bao, High-performance liquid chromatographic determination of histamine in biological samples: The cerebrospinal fluid challenge–A review, *Anal. Chim. Acta*, 2013, **774**, 1.
18 P. C. Wanniarachchi, K. U. Kumarasinghe and C. Jayathilake, Recent advancements in chemosensors for the detection of food spoilage, *Food Chem.*, 2024, **436**, 137733.
19 B. Wang, H. Jiang, R. Tang, Y. Tan, X. Xia and X. Zhang, Construction of histamine aptamer sensor based on Au NPs nanozyme for ultrasensitive SERS detection of histamine, *J. Food Compos. Anal.*, 2023, **120**, 105337.
20 R. Meng, L. R. Chen, M. L. Zhang, W. K. Cai, S. J. Yin, Y. X. Fan, T. Zhou, Y. H. Huang and G. H. He, Effectiveness and Safety of histamine H_2 receptor antagonists: an umbrella review of meta-analyses, *J. Clin. Pharmacol.*, 2023, **63**(1), 7–20.
21 B. P. Correia, M. P. Sousa, C. E. Sousa, D. Mateus, A. I. Sebastião, M. T. Cruz, A. M. Matos, A. C. Pereira and F. T. Moreira, Development of colorimetric cellulose-based test-strip for the rapid detection of antibodies against SARS-CoV2 virus, *Cellulose*, 2022, **29**(17), 9311–9322.
22 R. Ebrahimi, M. Hasanzadeh, N. Shadjou and A. Nilghazi, Aptasensing of rivaroxaban in human plasma using KCC-1-NH-CS_2 modified conductive nano-ink: A new biosensor, *Microchem. J.*, 2024, **207**, 111744.
23 F. Kvasnička, S. Kavková and A. Honzlová, Electrophoretic determination of histamine, *J. Chromatogr. A*, 2019, **1588**, 180–184.
24 Y. Fan, R. Yu, Y. Chen, Y. Sun, G. I. Waterhouse and Z. Xu, A capillary electrophoresis method based on molecularly imprinted solid-phase extraction for selective and sensitive detection of histamine in foods, *Molecules*, 2022, **27**(20), 6987.
25 L. Vitali, A. C. Valese, M. S. Azevedo, L. V. Gonzaga, A. C. Costa, M. Piovezan, J. P. Vistuba and G. A. Micke, Development of a fast and selective separation method to determine histamine in tuna fish samples using capillary zone electrophoresis, *Talanta*, 2013, **106**, 181–185.
26 M. Sato, Z. H. Tao, K. Shiozaki, T. Nakano, T. Yamaguchi, T. Yokoyama, N. Kan-No and E. Nagahisa, A simple and rapid method for the analysis of fish histamine by paper electrophoresis, *Fish. Sci.*, 2006, **72**, 889–892.
27 A. Dang, J. J. Pesek and M. T. Matyska, The use of aqueous normal phase chromatography as an analytical tool for food analysis: Determination of histamine as a model system, *Food chem.*, 2013, **141**(4), 4226–4230.
28 M. A. Munir, M. M. Mackeen, L. Y. Heng and K. H. Badri, Study of histamine detection using liquid chromatography and gas chromatography, *ASM Sci. J.*, 2021, **16**, 1–9.
29 B. K. Jinadasa, G. D. Jayasinghe and S. B. Ahmad, Validation of high-performance liquid chromatography (HPLC) method for quantitative analysis of histamine in fish and fishery products, *Cogent Chem.*, 2016, **2**(1), 1156806.
30 B. K. Jinadasa, G. D. Jayasinghe and S. B. Ahmad, Validation of high-performance liquid chromatography (HPLC) method for quantitative analysis of histamine in fish and fishery products, *Cogent Chem.*, 2016, **2**(1), 1156806.
31 S. B. Patange, M. K. Mukundan and K. A. Kumar, A simple and rapid method for colorimetric determination of histamine in fish flesh, *Food control*, 2005, **16**(5), 465–472.
32 J. Bi, C. Tian, G. L. Zhang, H. Hao and H. M. Hou, Detection of histamine based on gold nanoparticles with dual sensor system of colorimetric and fluorescence, *Foods*, 2020, **9**(3), 316.
33 S. Li, T. Zhong, Q. Long, C. Huang, L. Chen, D. Lu, X. Li, Z. Zhang, G. Shen and X. Hou, A gold nanoparticles-based molecularly imprinted electrochemical sensor for histamine specific-recognition and determination, *Microchem. J.*, 2021, **171**, 106844.

34 N. Nontipichet, S. Khumngern, J. Choosang, P. Thavarungkul, P. Kanatharana and A. Numnuam, An enzymatic histamine biosensor based on a screen-printed carbon electrode modified with a chitosan–gold nanoparticles composite cryogel on Prussian blue-coated multi-walled carbon nanotubes, *Food Chem.*, 2021, **364**, 130396.

35 S. Xu, F. Wu, F. Mu and B. Dai, The preparation of Fe-based peroxidase mimetic nanozymes and for the electrochemical detection of histamine, *J. Electroanal. Chem.*, 2022, **908**, 116088.

36 M. A. Sahudin, L. L. Tan, M. S. Su'ait, N. H. Abd Karim and M. M. Mackeen, Regenerable and selective histamine impedimetric sensor based on hydroxyl functionalised Schiff base complex electrode, *Electrochim. Acta*, 2021, **379**, 138186.

37 B. Shkodra, B. Demelash Abera, G. Cantarella, A. Douaki, E. Avancini, L. Petti and P. Lugli, Flexible and printed electrochemical immunosensor coated with oxygen plasma treated SWCNTs for histamine detection, *Biosensors*, 2020, **10**(4), 35.

38 N. Kumar and R. N. Goyal, Silver nanoparticles decorated graphene nanoribbon modified pyrolytic graphite sensor for determination of histamine, *Sens. Actuators B: Chem.*, 2018, **268**, 383–391.

39 A. Veseli, M. Vasjari, T. Arbneshi, A. Hajrizi, Ľ. Švorc, A. Samphao and K. Kalcher, Electrochemical determination of histamine in fish sauce using heterogeneous carbon electrodes modified with rhenium (IV) oxide, *Sens. Actuators B: Chem.*, 2016, **228**, 774–781.

40 I. M. Apetrei and C. Apetrei, Amperometric biosensor based on diamine oxidase/platinum nanoparticles/graphene/chitosan modified screen-printed carbon electrode for histamine detection, *Sensors*, 2016, **16**(4), 422.

41 M. B. Gumpu, N. Nesakumar, S. Sethuraman, U. M. Krishnan and J. B. Rayappan, Development of electrochemical biosensor with ceria–PANI core–shell nano-interface for the detection of histamine, *Sens. Actuators B: Chem.*, 2014, **199**, 330–338.

42 V. Carralero, A. González-Cortés, P. Yáñez-Sedeño and J. M. Pingarron, Pulsed amperometric detection of histamine at glassy carbon electrodes modified with gold nanoparticles, *Electroanalysis*, 2005, **17**(4), 289–297.

43 D. Telsnig, K. Kalcher, A. Leitner and A. Ortner, Design of an amperometric biosensor for the determination of biogenic amines using screen printed carbon working electrodes, *Electroanalysis*, 2013, **25**(1), 47–50.